Finite Elements in Analysis and Design 47 (2011) 1223–1231

Contents lists available at ScienceDirect

Finite Elements in Analysis and Design

journal homepage: www.elsevier.com/locate/finel

Fast iterative solvers for thin structures

Vikalp Mishra, Krishnan Suresh *

Department of Mechanical Engineering, University of Wisconsin, 1513 University Avenue, Madison, WI 53706, USA

ARTICLE INFO

Article history:
Received 27 January 2011
Received in revised form
18 April 2011
Accepted 24 May 2011
Available online 30 June 2011

Keywords:
Beams
Plates
Finite element analysis
Iterative
Pre-conditioners
Euler–Bernoulli
Kirchhoff–Love

ABSTRACT

For very large systems of equations arising from 3D finite element formulation, pre-conditioned iterative solvers are preferred over direct solvers due to their reduced memory requirements. However, in the finite-element analysis of thin structures such as beam and plate structures, iterative solvers perform poorly due to the presence of poor quality elements. In particular, their efficiency drops significantly with increase in the aspect ratio of such structures.

In this paper, we propose a dual-representation based multi-grid framework for efficient iterative analysis of thin structures. The proposed iterative solvers are relatively insensitive to the quality of the elements since they exploit classical beam and plate theories to spectrally complement 3D finite element analysis. This leads to significant computational gains, as supported by the numerical experiments.

1. Introduction

Thin structures such as beams, plates and shells find a wide variety of applications across many disciplines including civil, automotive, aerospace, MEMS, etc. Fig. 1 illustrates examples of such thin structures.

Currently, three different strategies exist for the structural analysis of such thin structures [1]:

1. *Dimensionally reduced analysis*: This is a traditional approach where the thin structure is first dimensionally reduced to 1D (for beams) or 2D (for plates and shells). The reduced problem is then solved relying on lower-dimensional theories such as Euler–Bernoulli (for beams) and Reissner–Mindlin (for plates/shells) [2,3]. Though highly efficient, such methods are hard to integrate within today's 3D design environment, and with increased geometric complexity, automated construction of reduced models can be cumbersome [4,5]. Further, the inability of these reduced models to capture stress concentration and other 3D effects limits their use in certain applications.
2. *3D finite-element analysis*: When accurate stress prediction is critical and/or when 3D CAD integration is important, one must rely on a full 3D structural analysis. Among 3D methods of analysis, finite element analysis (FEA) is most popular because of its ability to capture complex geometric features and ease of implementation. However, use of 3D FEA to analyze thin structures entails a high level of discretization to avoid Poisson-locking and ill-conditioning [1,6]. This, in turn, leads to a large system of equations [1,7,8] that can be computationally challenging to solve. We shall discuss methods for solving such large systems of equations in a later section as this is the primary focus of this paper.
3. *Alternate 3D methods*: Alternate formulations have also been proposed; these include: (1) solid shell, where relatively low order shape functions are used across the thickness to overcome ill-conditioning [9,10]; (2) reduced integration techniques that employ lower-order polynomials for computational efficiency [11–14]; and (3) hybrid or mixed formulations, where both displacement and stresses are used as free variables [1,12,15]. Some of the limitations of these methods are discussed, for example, in [16].

   In this paper, we propose a fourth strategy that combines the simplicity of dimensionally reduced models and the generality of 3D FEA:
4. *(Proposed) dual-representation based 3D analysis*: In the proposed method, we rely on standard 3D FEA for assembling the linear systems of equations. However, these equations are solved with the help of classical reduced dimension models. This is achieved by combining the multi-grid idea [17,18] with the recently proposed dual-representation method for thin-structure analysis [16,19–23]. We show that the proposed method leads to rapid convergence, and the computational cost is relatively insensitive to the element quality; this is in contrast to standard pre-conditioners. Further, we illustrate

* Corresponding author. Tel.: +1 608 262 3594; fax: +1 608 265 2316.
E-mail address: suresh@engr.wisc.edu (K. Suresh).

0168-874X/$ - see front matter © 2011 Elsevier B.V. All rights reserved.
doi:10.1016/j.finel.2011.05.010

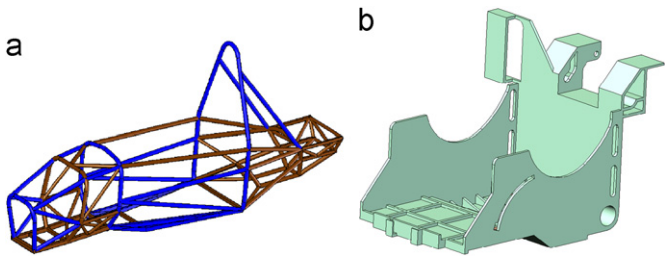

Fig. 1. Examples of thin structures: (a) a Chassis structure and (b) printer-housing.

that the proposed method can be combined with standard pre-conditioners to further improve computational efficiency. Finally, since the method is based on 3D FEA, it can accurately capture 3D stress concentration, unlike classical dimension reduction methods.

The rest of the paper is organized as follows. In Section 2, we present background material related to pre-conditioning and multi-grid. In Section 3, the proposed framework and the underlying concepts of dual-representation are discussed. In Section 4, numerical examples are presented to support the proposed methodology, followed by conclusion and future work in Section 5.

2. Background

2.1. Pre-conditioned iterative methods

As it is well known, accurate 3D FEA of thin structures entails high level of discretization, resulting in a large system of equations of the form:

$$Kd = q \tag{2.1}$$

These large linear systems put severe memory requirements on direct solution techniques [8,24,25]. Thus, they are typically solved using Krylov subspace based iterative methods, like conjugate gradient (CG), minimum residual (MINRES), bi-conjugate gradient (BCG), quasi-minimum residual (QMR), etc [25], together with appropriate pre-conditioners.

A pre-conditioner is a matrix or a method that transforms the original system of equations to one that has the same solution, but has more favorable spectral properties [25,26]. For example, if M is a non-singular matrix that approximates the stiffness matrix K in a spectral sense, then it can be used as a pre-conditioner by multiplying the system in Eq. (2.1) with its inverse from the left [24]:

$$M^{-1}Kd = M^{-1}q \tag{2.2}$$

There are several types of pre-conditioners available today, and among them incomplete factorization based pre-conditioners are most widely used; these include incomplete Cholesky (IC) for symmetric positive definite stiffness matrices, and incomplete LU for non-symmetric or indefinite stiffness matrices [24,25,27,28]. Alternate formulations based on fixed fill-in or drop-tolerance are possible, but require *a priori* prediction of the fill-in or drop-tolerance parameters, making it difficult to predict the required storage and associated benefits for a given problem [29].

While IC with no-fill, i.e., IC(0), can typically reduce the computational cost during iterative analysis, its efficiency drops rapidly as the element quality drops. As a specific example, Fig. 2 illustrates the number of iterations required to solve a simple I-beam problem via IC(0) based pre-conditioned MINRES (p-MINRES). For the analysis in Fig. 2, the number of 3D elements was kept approximately

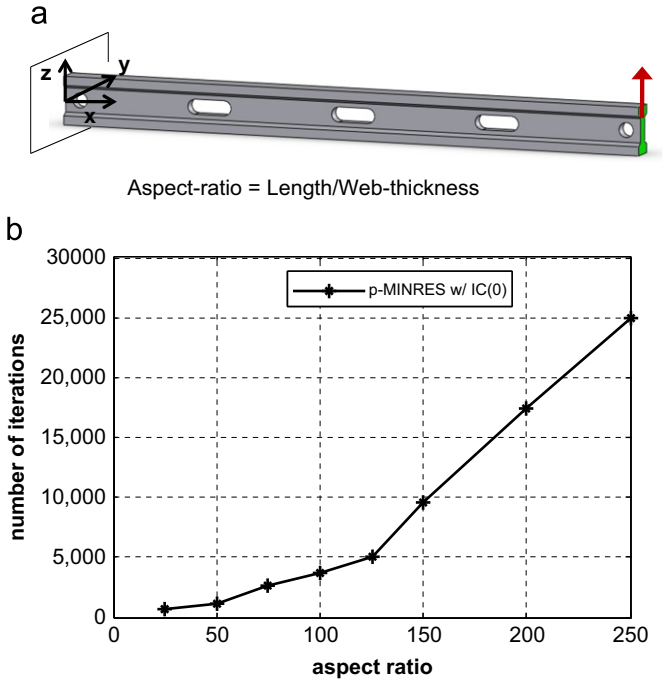

Fig. 2. Performance of IC(0) pre-conditioner: (a) a thin structure problem and (b) performance of IC(0).

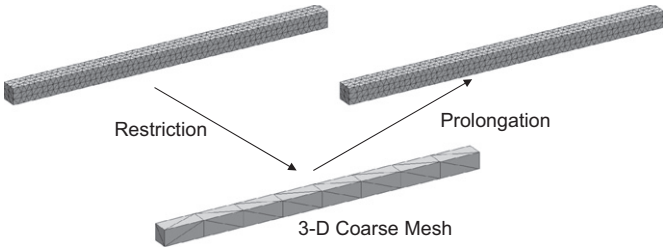

Fig. 3. Correction scheme using 3D coarse mesh.

constant for different aspect ratios, i.e., the element quality dropped with increasing aspect ratio. The iterations were terminated when six orders of magnitude drop when initial residual was achieved.

As one can observe, the computational cost of these preconditioned iterative solvers increases rapidly with the aspect ratio of the structure.

2.2. The multi-grid method

An alternate and powerful 'pre-conditioner' is based on the multi-grid concept. Since multi-grid plays an important role in this paper, we provide a brief overview of the method; additional details can be found, for example, in [18].

In the multi-grid method, the Krylov methods are accelerated using grids of varying densities. This exploits the fact that low-frequency error components that are not eliminated by a Krylov 'smoothener' can be projected onto a coarser grid, where it appears as high frequency, and can easily be smoothed out. The process is repeated until the coarsest grid on which direct solution or smoothing is performed. Thereafter the results are prolonged back up the sequence of grids to the finest level on which the solution is sought [8,17,18]. A 2level multi-grid is depicted in Fig. 3.

The stability and efficiency of the multi-grid method depends on the choice of prolongation and restriction operators.

Additionally, the performance also depends on the selection of the coarse mesh, and on the algebraic technique used for constructing the coarse stiffness matrix in the case of algebraic multi-grid method [17,18,30].

Multi-grid methods have been proposed for linear elasticity problems and for thin structures [8,31–35]. However, as mentioned earlier, a coarse mesh based multi-grid is prone to Poisson locking and ill-conditioning, which undermines the quality of the coarse grid correction.

The deterioration in the coarse grid approximation demands more correction steps degrading the performance of the method, especially with the decrease in element quality [36]. Hence, an alternate formulation was proposed by Ruge and Brandt [36], which used a composite grid (3D or 2D with 1D) with auxiliary functions specified on 1D nodes. These auxiliary functions were defined to capture the shear stress at 1D nodes. The method was limited to straight boundary domains, required use of structured mesh and involved complex computations for 1D auxiliary functions, making a 3D implementation fairly difficult, also acknowledged by the authors [36].

A new approach for thin-structure analysis was proposed by Mikulinsky [37], which employed a 1D mesh for coarse grid correction when solving 2D or 3D beam problems using finite difference method. He started with 3D (or 2D) equations of elasticity and ignored terms containing derivatives with respect to the thickness-direction coordinate. Though the method was capable of handling curved boundaries, it was limited to boundaries, which could be represented by continuous functions, making it difficult to account for features like holes, cuts, stiffeners, etc. Moreover, it required a structured mesh, as in [36], and before applying 1D correction, the fine mesh had to be coarsened to a level where there were only three nodes along beam thickness, limiting the efficiency of the overall process.

3. Proposed methodology

3.1. Proposed concept

The work presented in this paper is based on the idea of using lower dimensional correction. However, instead of explicitly modifying 3D equations of elasticity as in [37], we use classical dimension reduction theories in conjunction with dual-representation for a one-time construction of lower dimension stiffness matrix, prolongation and restriction operators.

The use of lower dimension physics helps avoid Poisson locking and ill-conditioning, while dual-representation helps in capturing geometric complexity. The concept is illustrated via a two-level correction step in Fig. 4.

3.2. Dual representation: beams

The dual-representation method for beams as explained in [22] exploits 1D beam physics, but is implemented within a 3D environment by appealing to divergence theorem. To understand this, let us consider a 3D beam of length L and an arbitrarily varying cross-section $A(x)$, oriented along the x-direction, as in Fig. 2. Also assume that to capture generalized Euler–Bernoulli beam kinematics [3,19]

$$u(x,y,z) \approx u_0(x) - y\frac{\partial v_0}{\partial x} - z\frac{\partial w_0}{\partial x}$$

$$v(x,y,z) \approx v_0(x)$$

$$w(x,y,z) \approx w_0(x) \tag{3.1}$$

we use a 11-degrees-of-freedom (DOFs) beam element comprising of bending and stretching [19], as in Fig. 5, where L_e is the element length.

If bending is captured via Hermite cubic polynomials [12], $H(0 \le t \le 1;\ t = x/L_e)$, and stretching via second order Lagrange polynomials [38], $\ell^2(-1 \le \xi \le 1);\ \xi = x/L_e$, then the components of the Euler–Bernoulli beam stiffness matrix can be given by splitting the 3D domain, say Ω as $[0,L] \otimes A(x)$ [1,12,38]:

$$(K_{EB})_{ij} = \int_0^{L_e} \int_{A(x)} E \left\{ \begin{matrix} (N^u_{i,x} - yN^v_{i,xx} - zN^w_{i,xx})\ldots \\ \ldots(N^u_{j,x} - yN^v_{j,xx} - zN^w_{j,xx}) \end{matrix} \right\} dA\,s\,dx \tag{3.2}$$

where $(i,j = 1\ldots13)$ and

$$N^u = \left[\ell^2(\xi) \quad 0_{1\times8} \right]$$

$$N^v = \left[0_{1\times3} \quad H(t) \quad 0_{1\times4} \right]$$

$$N^w = \left[0_{1\times3} \quad 0_{1\times4} \quad H(t) \right] \tag{3.3}$$

such that 3D displacements are approximated as

$$u_0 \approx N^u d_{1D}; \quad v_0 \approx N^v d_{1D}; \quad w_0 \approx N^w d_{1D} \tag{3.4}$$

for

$$d_{1D} = \left\{ u_1,\ u_3,\ u_2,\quad v_1,\ \theta_1^z, v_2,\ \theta_2^z,\quad w_1,\ \theta_1^y, w_2,\ \theta_2^y \right\} \tag{3.5}$$

If $A(x)$ is constant or sufficiently simple, then Eq. (3.2) can be evaluated analytically. However, with the increase in geometric complexity analytical evaluation becomes more challenging.

Instead of splitting the 3D domain as above, dual-representation method appeals to divergence theorem, which states that for any differentiable vector function $\vec{F}$ [39]

$$\int_\Omega \nabla \cdot \vec{F}\, d\Omega = \int_{\partial\Omega} \vec{F} \cdot \vec{n}\, d\Gamma \tag{3.6}$$

where $\vec{n}$ is the boundary normal and $\partial\Omega$ is the boundary of Ω. Hence, we need to find a function $\vec{F}$, such that $\nabla \cdot \vec{F}$ is exactly equal

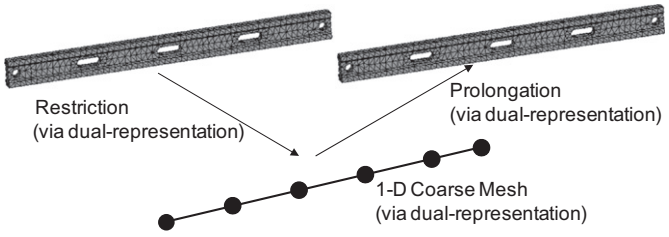

Fig. 4. Correction scheme using dual-representation based 1D beam formulation.

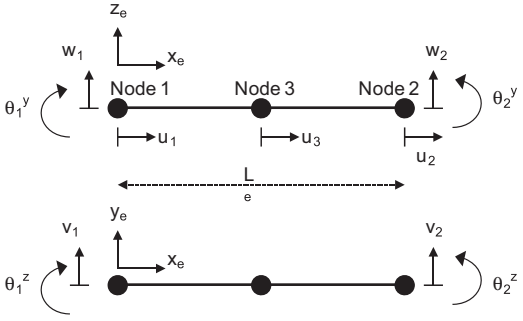

Fig. 5. A 11-DOF beam element [21].

to the integrand in Eq. (3.2). One such possibility is (see [22])

$$\vec{F} = E\begin{bmatrix} z\begin{pmatrix} N^u_{i,x}N^u_{j,x} + y^2(N^v_{i,xx}N^v_{j,xx}) \\ -y(N^u_{i,x}N^v_{j,xx} + N^v_{i,xx}N^u_{j,x}) \end{pmatrix} \\ +\frac{z^2}{2}\begin{pmatrix} y(N^v_{i,xx}N^w_{j,xx} + N^w_{i,xx}N^v_{j,xx}) \\ -N^u_{i,x}N^w_{j,xx} - N^w_{i,xx}N^u_{j,x} \end{pmatrix} \\ +\frac{z^3}{3}(N^w_{i,xx}N^w_{j,xx}) \end{bmatrix}\vec{e}_z \tag{3.7}$$

where $\vec{e}_z$ is the unit vector along the z-direction.

This gives the dual-representation beam stiffness matrix as [22]

$$(K_{DR-beam})_{ij} = \int_{\partial\Omega} \vec{F}\cdot\vec{n}\, d\Gamma \tag{3.8}$$

Thus, for any given geometry, we can obtain a dual-representation beam stiffness matrix using simple boundary integration, where the integration needs to be performed only on the boundaries where $n_z \neq 0$ (n_z is the z-component of the boundary normal) [22]. Also note that for uniform cross-section geometries, dual representation gives exactly the same stiffness matrix as classical reduced dimension formulation, as shown in [22].

3.3. Dual representation: plates

An analogous dual-representation formulation for 3D plates can be given, based on the Kirchhoff–Love plate kinematics [3,16]:

$$\begin{aligned} u(x,y,z) &\approx -z\frac{\partial \tilde{w}_0}{\partial x} \\ v(x,y,z) &\approx -z\frac{\partial \tilde{w}_0}{\partial y} \\ w(x,y,z) &\approx \tilde{w}_0(x,y) \end{aligned} \tag{3.9}$$

If we assume a 2D discretization based on 12-DOF quad element from [40], such that

$$\tilde{w}_0(x,y) = S(\xi,\eta)d_{2D} \tag{3.10}$$

as in [16], we get the Kirchhoff–Love plate stiffness matrix as

$$K_{KL} = \int_\Omega B^T D B\, d\Omega = \int_\Omega z^2 \tilde{B}^T D \tilde{B}\, d\Omega \tag{3.11}$$

where D is a 3-by-3 constitutive matrix, B is the appropriate strain–displacement matrix [12] and $\tilde{B}$ is defined such that $B = z\tilde{B}$ [16].

Once again exploiting divergence theorem we can re-write the stiffness matrix of Eq. (3.11) as

$$K_{DR-plate} = \int_{\partial\Omega}\left[\frac{z^3}{3}\tilde{B}^T D\tilde{B}\right]\vec{e}_z\cdot\vec{n}\, d\sigma \tag{3.12}$$

Please note that for the simplicity of expression we have only considered bending in the above plate formulation; however, we can account for stretching in u and v via Q9 shape functions [12].

3.4. Prolongation and restriction operators

Since our correction step is based on lower dimension physics, the prolongation matrix should be defined in such a way that it aptly maps the lower dimension kinematic constraints to 3D nodal displacements.

Thus, based on the kinematics of Section 3.2, the displacements for a 3D beam node (x_i,y_i,z_i) can be given by

$$u_i = (N^u_i - y_i N^v_{i,x} - z_i N^w_{i,x})d_{1D}\, v_i = N^v_i d_{1D}\, w_i = N^w_i d_{1D} \tag{3.13}$$

This can be used to define the mapping for every 3D node as

$$\begin{aligned} P^u_{beam}(i,:) &= N^u_i - y_i N^v_{i,x} - z_i N^w_{i,x} \\ P^v_{beam}(i,:) &= N^v_i \\ P^w_{beam}(i,:) &= N^w_i \end{aligned} \tag{3.14}$$

which in turn gives us our beam prolongation and restriction operators as follows [19,20]:

$$P_{beam} = \begin{bmatrix} P^u_{beam} & P^v_{beam} & P^w_{beam} \end{bmatrix}^T; \quad R_{beam} = P^T_{beam} \tag{3.15}$$

In a similar manner the prolongation and restriction operators for a 3D plate node can be constructed. For the kinematics of Eq. (3.9), the mapping analogous to Eq. (3.14) is

$$\begin{aligned} P^u_{plate}(i,:) &= -z_i S_{i,x} \\ P^v_{plate}(i,:) &= -z_i S_{i,y} \\ P^w_{plate}(i,:) &= S_i \end{aligned} \tag{3.16}$$

which gives the respective plate operators as [16]

$$P_{plate} = \begin{bmatrix} P^u_{plate} & P^v_{plate} & P^w_{plate} \end{bmatrix}^T; \quad R_{plate} = P^T_{plate} \tag{3.17}$$

3.5. Algorithm

Typically in a multi-grid setup the number of fine grid iterations pre- and post-coarse corrections are fixed a *priori*. For example, Mikulinsky fixes them at 1 and 2 [37], while various combinations are tested in [31,35]. However, as suggested in [18], the coarse-grid correction is most effective when high-frequency errors in the fine grid have been eliminated. This forms the basis of our criteria for switching between 3D and lower dimension mesh.

Suppose we are using a residual minimization Krylov iterative method like MINRES or QMR. The basis of these algorithms suggests that the residual should drop with every iteration [25]. If the residual stagnates over successive iterations, we can conclude that the iterative method is struggling and needs assistance in the form of coarse-grid or lower-dimension correction, later being the case for our implementation. A similar analogy may be used for energy minimization methods, like CG, using energy stagnation criteria.

For implementation we define a stagnation parameter (SP) and stagnation limit (SL). We start with 3D iterations and apply correction whenever relative residual is less than SP for three consecutive iterations (we call this a 'stagnation point'). If the 3D residual after correction is less than pre-correction 3D residual we continue with 3D iterations, else we reduce SP by some factor, say f, discard correction and continue with 3D iterations till new 'stagnation point' is reached. At any point in this adaptive process if SP becomes less than SL, we conclude that the lower dimension correction is not helping 3D iterative process; hence, stop applying corrections beyond that point. The algorithm is illustrated via a flowchart in Fig. 6.

4. Numerical examples

Since the problems considered in this paper lead to symmetric-positive-definite matrices, we shall use incomplete Cholesky (IC) pre-conditioners for comparison purposes. In particular, we will use IC with no-fill, IC(0).

For all numerical examples, we assume that Young's modulus $E = 2\times10^{11}$, Poisson ratio $\nu = 0.33$, load per unit area is $q_o = 1$, SP $= 10^{-8}$ and SL $= 10^{-16}$, unless otherwise stated. Further, we use MINRES iterative method and convergence is assumed when six orders of magnitude drop in residual is achieved.

Unless otherwise specified, a 20-beam element mesh is used for 1D beam discretization and a 12-by-12 quad element mesh is used for 2D plate discretization, for construction of corresponding dual representation 1D beam or 2D plate stiffness matrix, as well as prolongation and restriction matrices. The 3D model is discretized using sufficiently large number of tetrahedral elements, such that standard FEA does not "lock".

4.1. Example 1: Element quality insensitivity

In this first experiment, we consider a cantilevered rod fixed on the left end, and with a tip load of q_o, on the right, as shown in Fig. 7. The 3D mesh used for this problem has roughly 60,000 DOFs (about 18,000 tet-elements) for all aspect ratios. Thus, with increasing aspect ratio, the element quality drops, with minimum 3D mesh quality of 0.45 for aspect ratio of 10 and 0.3 for aspect of 50. The convergence plots for various aspect ratios are shown in Fig. 7.

It is evident that with the increase in aspect ratio the proposed method performs much better than p-MINRES with IC(0), and the combined implementation is nearly insensitive to element quality.

Similar behavior is seen for a uniformly loaded thin plate with built-in edges, as shown in Fig. 8. The 3D mesh for these examples has approximately 130,000 DOFs (about 37,000 tet-elements, with minimum element quality or 0.3 and 0.21, and average 3D mesh quality of 0.82 and 0.74).

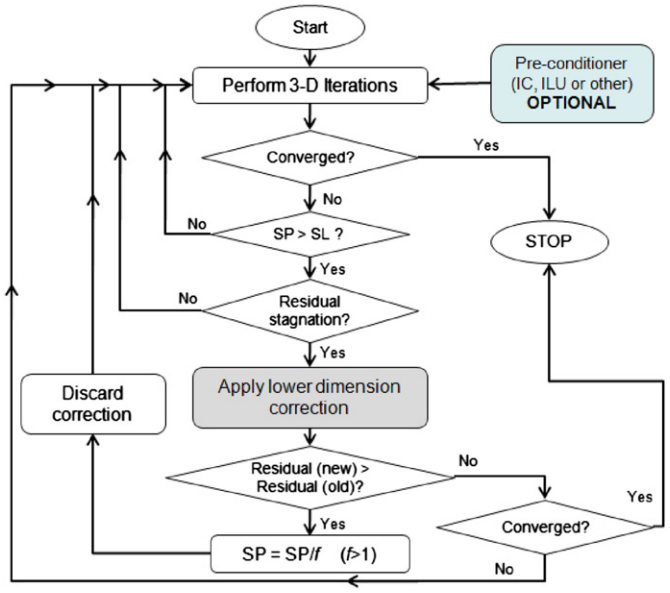

Fig. 6. Proposed algorithm.

4.2. Example 2: Complex geometry

To demonstrate the capability of our method in handling complex geometry, we re-visit the I-beam of Fig. 2. Once again 20 1D beam elements are used for the computation of beam stiffness and projection matrices. The number of iterations required for each method is shown in Fig. 9. Once again, the advantage of the proposed method is evident. The 3D mesh used for this case comprises of about 33,500 tet-elements, with average mesh quality dropping from 0.90 to 0.68 with the increase in aspect ratio from 25 to 250.

A plate example having a pattern of rectangular shaped protrusions with filleted sections (on one face) is also presented in Fig. 10. It is non-trivial to model such a plate using reduced dimension methods; however, dual representation captures the impact of features, and leads to rapid convergence as shown in Fig. 10. The plate is assumed to have built-in edges and has a uniform load of q_o, on the face without any pattern (illustrated in Fig. 10). The 3D mesh of this problem contained roughly 41,000 tet-elements with 150,000 DOFs and average 3D mesh quality of 0.76.

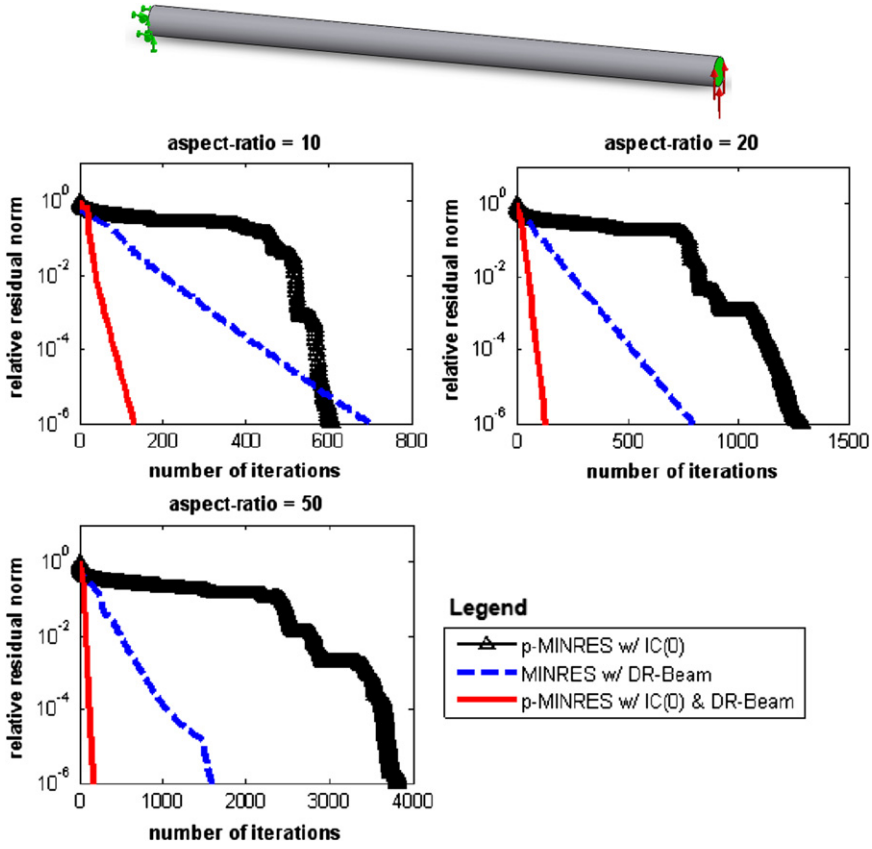

Fig. 7. Bending of a rod of different aspect ratios.

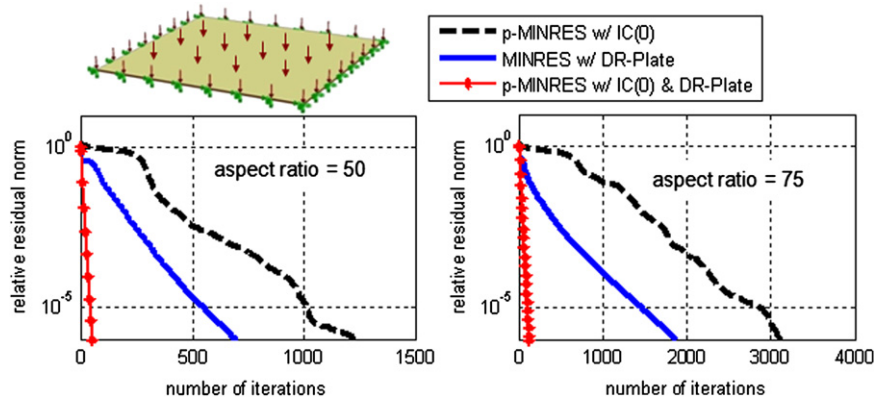

Fig. 8. Problem of thin plate with built-in edges.

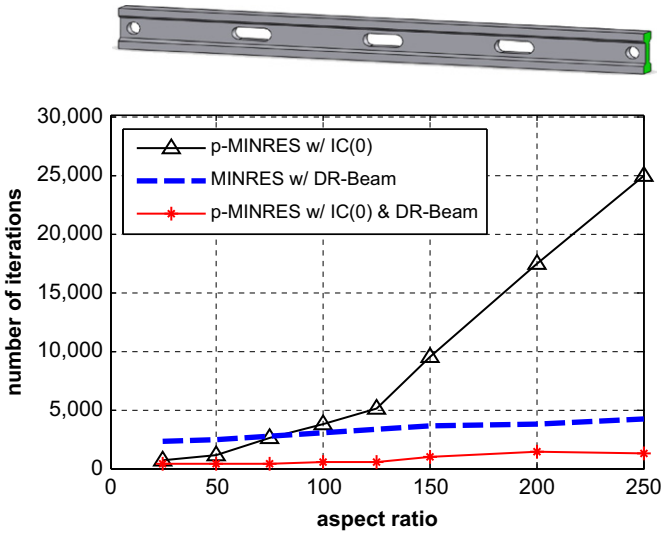

Fig. 9. Performance on complex beam geometry.

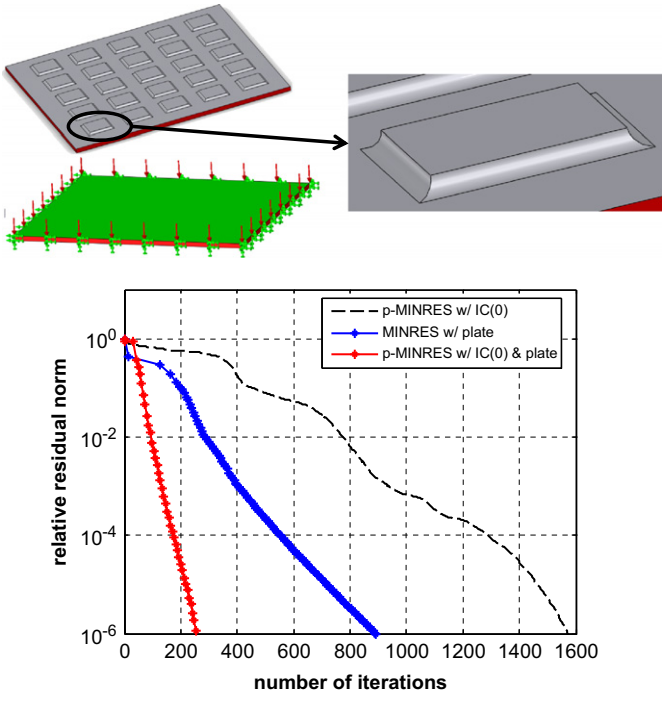

Fig. 10. Performance on 3D plate with features.

4.3. Example 3: Why dual representation?

To assert the significance of capturing actual 3D geometry for lower dimension correction, and to highlight the importance of dual representation in the proposed framework, we consider a tapered cantilevered rod, fixed on the left end and having a tip load of q_o on the right end. For 1D stiffness matrix formulation, we use two methods: (1) dual representation (DR), which accounts for actual geometry, and (2) Euler–Bernoulli (EB), assuming average uniform cross-section across the beam length. A comparison of the performance of DR and EB based correction is given in Fig. 11 for the tapered beam of aspect ratios 10 and 15.

Clearly dual-representation formulation plays a vital role in the correction process. For this example, we used a 3D mesh with about 32,000 tet-elements, with an average quality of 0.82 for aspect ratio of 10, and 0.77 for aspect ratio of 15.

4.4. Example 4: Capturing 3D stress

Since the proposed method is based on 3D FEA, it is capable of capturing stress concentration, and it does so more efficiently.

To illustrate this, we consider a tip-loaded t-shaped cantilevered beam, fixed on the left end and having a tip load of q_o on the right end (similar to that for the problem of Section 4.3). The cross-section of the beam is shown in Fig. 12. The length of the beam was fixed at 200 units, so that the number of iterations required for residual convergence by the methods "p-MINRES w/IC(0)" and "MINRES w/ DR-Beam" was approximately the same. Approximately 34,000 tet-elements were used to model the problem with minimum element quality of 0.25 and average quality of 0.8.

As illustrated in Fig. 12(b), the 3D stress error with respect to final 3D solution drops much faster for the proposed method. For example, after about 600 iterations, the relative error in stress is less than 10^{-4} for the proposed method, while that for the pre-conditioned iterative method is almost 1. Hence, in typical structural analysis applications where stress is the quantity of interest one can terminate iterations much earlier.

4.5. Example 5: Beam structure

The proposed method can further be extended to beam structures, for example, to solve the problem of a 3D L-shaped solid rod with boundary conditions as in Fig. 13(a) (where the ratio of cross-sectional diameter to length for each arm is 20).

For an equivalent 1D beam model we use a two-beam 1D structure shown in Fig. 13(b), and discretize each arm with 4 beam elements. The 3D discretization had about 40,000 tet-elements with minimum element quality of 0.42 and average quality of 0.83.

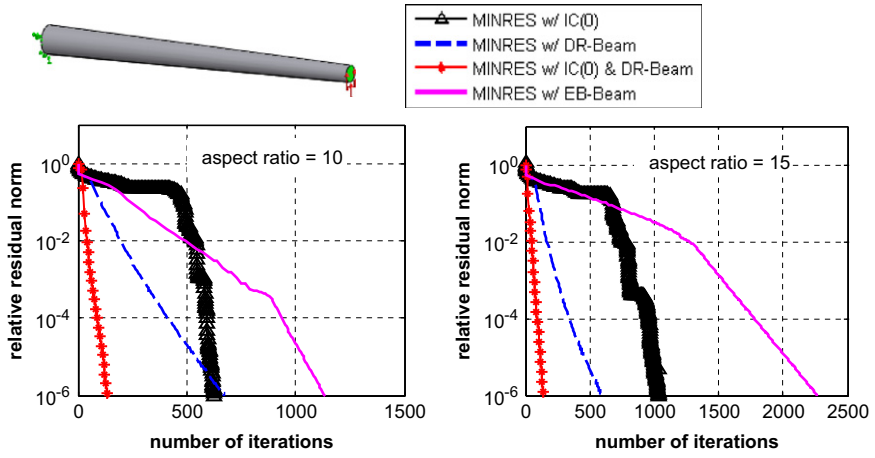

Fig. 11. Tapered-rod: comparison of Euler–Bernoulli (EB) with dual representation (DR).

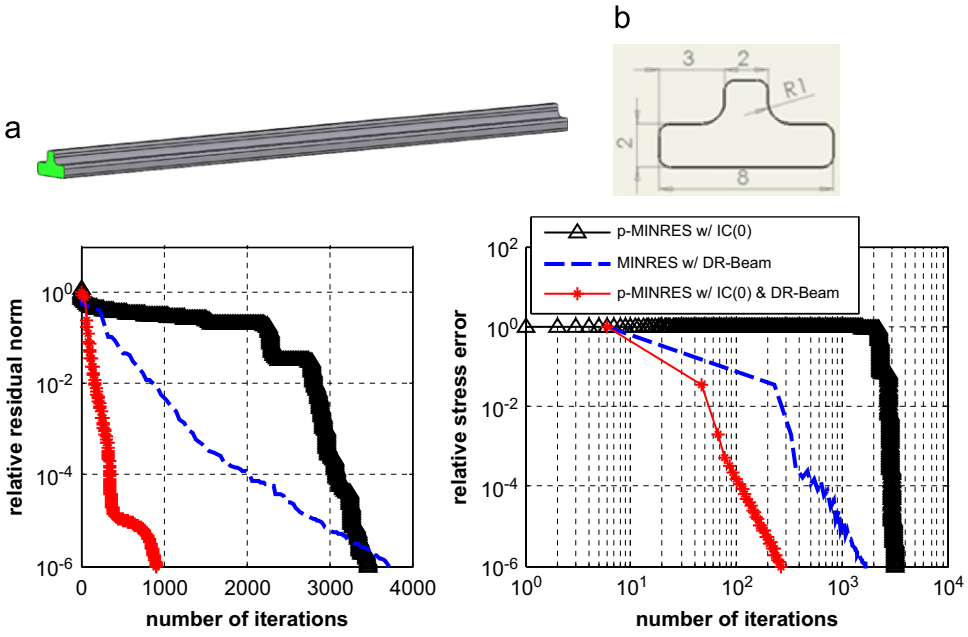

Fig. 12. Capturing 3D von Mises stress error: proposed versus pre-conditioned iterative method (total iterations for convergence ≈ 3400).

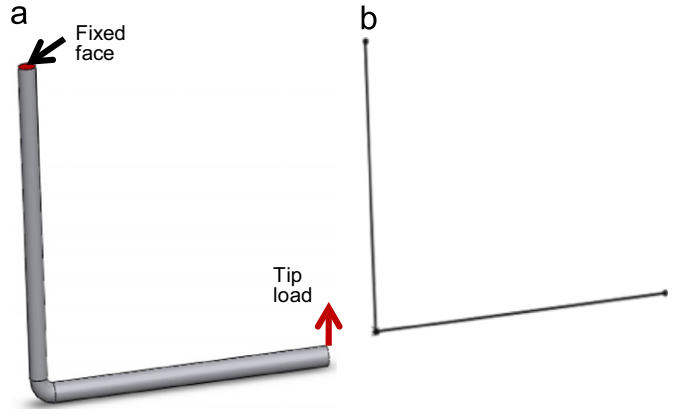

Fig. 13. (a) L-shaped rod with curved junction; (b) 1D model for dual-representation formulation.

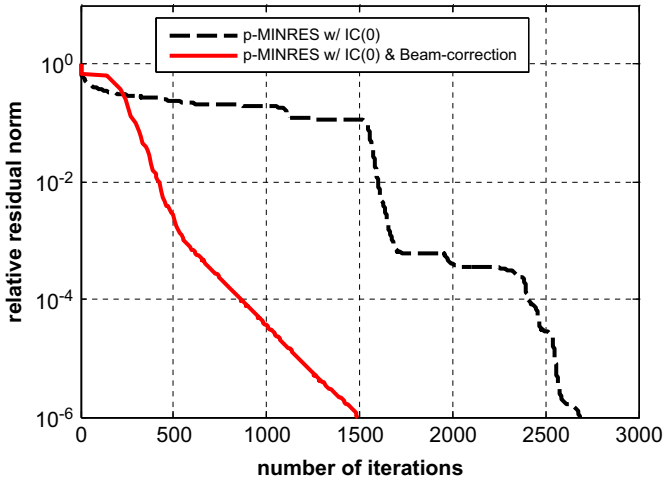

Fig. 14. Convergence profile for L-shaped rod.

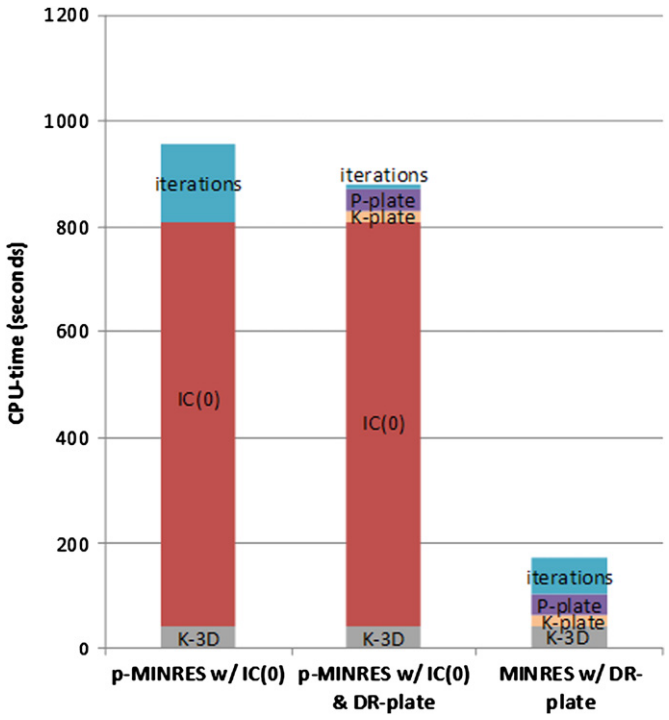

Fig. 15. CPU time comparison.

The corresponding convergence profile is shown in Fig. 14, where we compare p-MINRES with and without dual-representation based beam correction. Use of a curved beam might lead to faster convergence.

4.6. *Example 6: Computational efficiency*

To illustrate that the proposed method is indeed computationally efficient compared to a standard pre-conditioned iterative solver, in this section, we present in Fig. 15 a computational-time comparison for the uniformly loaded plate of Fig. 8.

The labels used in Fig. 15 are as follows:

- *K-3D*: time taken to assemble the 3D finite element stiffness matrix computation;
- *IC(0)*: time taken to compute the incomplete Cholesky factorization;
- *K-plate*: time taken to compute the dual-representation 2D plate stiffness matrix, using the Kirchhoff–Love plate theory;
- *P-plate*: time taken to assemble the projection matrix; and
- *Iterations*: time taken for the iterative process to converge, using either IC(0), dual representation or both.

The work was carried out using Matlab R2009b on a 64-bit Windows platform with Intel Core 2 Duo process of 3.17 GHz and 3 GB RAM, when no other process was executed.

Clearly, the proposed method is much faster than the incomplete factorization scheme, where the bottleneck is the incomplete factorization process. The main reason behind this is that the incomplete factorization is based on some form of Gauss elimination, which involves multiplicative operations on large 3D matrices, while the dual-representation formulation involves simple linear node-wise summation.

5. Conclusion

In this paper, we have described a dual-representation based multi-grid framework for rapid iterative analysis of thin structures. The proposed scheme exploits the strengths of a 3D FEA, as well as lower-dimension models to improve the computational efficiency of standard iterative solvers. The method as illustrated for beams and plates shows significantly better convergence, especially with drop in element quality. Further, the proposed method can be combined with existing pre-conditioners, resulting in further speed-ups. The proposed method also efficiently captures 3D stress concentration.

References

[1] O.C. Zienkiewicz, R.L. Taylor, The Finite Element Method for Solid and Structural Mechanics, 6th ed., Elsevier, 2005.
[2] E. Reissner, Reflections on the theory of elastic plates, Applied Mechanics Review 38 (1985) 1453–1464.
[3] C.M. Wang, J.N. Reddy, K.H. Lee, Shear Deformable Beams and Plates: Relationship to Classical Solutions, Elsevier Science, London, 2000.
[4] R.J. Donaghy, W. McCune, S.J. Bridgett, C.G. Armstrong, D.J. Robinson, R.M. McKeag, Dimensional reduction of analysis models, in: Proceedings of the 5th International Meshing Roundtable, 1996, Pittsburgh, Pennsylvania.
[5] K. Suresh, Automating the CAD/CAE dimensional reduction process, in: Proceedings of the 8th ACM Solid Modeling Conference, ACM, 2003, Seattle, USA.
[6] J. Dow, D.E. Byrd, The identification and elimination of artificial stiffening errors in finite elements, International Journal of Numerical Methods in Engineering 26 (3) (1988) 743–762.
[7] E.E. Ovtchinnikov, L.S. Xanthis, Effective dimensional reduction algorithm for eigenvalue problems for thin elastic structures: a paradigm in three dimensions, in: Proceedings of the National Academy of Sciences of the United States of America, vol. 97 (3), 2000, pp. 967–971.
[8] J.A. Mitchell, J.N. Reddy, A multilevel hierarchical preconditioner for thin elastic solids, International Journal of Numerical Methods in Engineering 43 (1998) 1383–1400.
[9] M. Bischoff, W.A. Wall, K.U. Beltzinger, E. Ramm, , Encyclopedia of Computational Mechanics, Volume 2: Solids and Structures, chapter 3. Models and finite elements for thin-walled structures, in: E. Stein, R. Borst., J.R. Hughes (Eds.), Encyclopedia of Computational Mechanics, vol. 2. Solids and Structures, John Wiley & Sons, 2004.
[10] A. Duster, H. Broker, E. Rank, The p-version of finite element method for three-dimensional curved thin walled structures, International Journal of Numerical Methods in Engineering 52 (7) (2001) 673–703.
[11] D. Braess, M. Kaltenbacher, Efficient 3D-finite-element-formulation for thin mechanical and piezoelectric structures, International Journal of Numerical Methods in Engineering (2007).
[12] R.D. Cook, D.S. Malkus, M.E. Plesha, Concepts and Applications of Finite Element Analysis, John Wiley, New York, 1989.
[13] A. Dorfmann, R.B. Nelson, Three-dimensional finite element for analysing thin plate/shell structures, International Journal of Numerical Methods in Engineering 38 (20) (1995) 3453–3482.
[14] H.T.Y. Yang, S. Saigal, A. Masud, R.K. Kapania, A survey of recent shell finite element, International Journal of Numerical Methods in Engineering 47 (1–3) (2000) 101–127.
[15] C.S. Jog, A 27-node hybrid brick and a 21-node hybrid wedge element for structural analysis, Finite Elements in Analysis and Design 41 (11,12) (2005) 1209–1232.
[16] V. Mishra, K. Suresh, Dual representation methods for efficient and automatable analysis of 3D plates, ASME International Journal of Computer & Information Science in Engineering 10 (4) (2010) 041002 (11 pp.).
[17] S.F. McCormick (Ed.), Multigrid Methods, SIAM, 1987.
[18] W.L. Briggs, V.E. Henson, S.F. McCormick, A Multigrid Tutorial, 2nd ed., SIAM, 2000.
[19] K. Jorabchi, J. Danczyk, K. Suresh, Algebraic Reduction of beams for CAD-integrated analysis, CAD 42 (9) (2010) 88–816.
[20] K. Jorabchi, J. Danczyk, K. Suresh, Efficient and automated analysis of potentially slender structures, Journal of Computing and Information Science in Engineering 9 (4) (2009) 041001 (9 pp.).
[21] K. Jorabchi, K. Suresh, Nonlinear algebraic reduction for snap-fit simulation, Journal of Mechanical Design 131 (2009) 6.
[22] W.A. Samad, K. Suresh, CAD-integrated analysis of 3-D beams: a surface-integration approach, Engineering with Computers (2010) (Online first).
[23] V. Mishra, K. Suresh, A dual-representation strategy for the virtual assembly of thin deformable objects, Virtual Reality (2009) (Online first).
[24] M. Benzi, Preconditioning techniques for large linear systems: a survey, Journal of Computational Physics 182 (2002) 418–477.
[25] Y. Saad, Iterative Methods for Sparse Linear Systems, 2nd ed., SIAM, 2003.
[26] R. Barrett, et al., Templates for the Solution of Linear Systems: Building Blocks for Iterative Methods, SIAM Press, Philadelphia, 1993.
[27] V. Simoncini, D.B. Szyld, Recent computational developments in Krylov subspace methods for linear systems, Numerical Linear Algebra With Applications 141 (2007) 1–59.
[28] M. Benzi, M. Tuma, A robust incomplete factorization preconditioner for positive definite matrices, Numerical Linear Algebra With Applications 10 (2003) 385–400.

[29] M.T. Jones, P.E. Plassmann, An improved incomplete Cholesky factorization, ACM Transactions on Mathematical Software 21 (1) (1995) 5–17.
[30] K. Stüben, A review of algebraic multigrid, Journal of Computational and Applied Mathematics 128 (2001) 281–309.
[31] P.S. Sumant, A.C. Cangellaris, N.R. Aluru, A node-based agglomeration AMG solver for linear elasticity in thin bodies, Communications in Numerical Methods in Engineering 25 (2009) 219–236.
[32] A.H. Baker, T.V. Kolev, U.M. Yank, Improving algebraic multigrid interpolation operators for linear elasticity problems, Numerical Linear Algebra With Applications 17 (2010) 495–517.
[33] E. Karer, J.K. Kraus, Algebraic multigrid for finite element elasticity equations: determination of nodal dependence via edge-matrices and two-level convergence, International Journal for Numerical Methods in Engineering (2010).
[34] M. Griebel, D. Oeltz, M.A. Schweitzer, An algebraic multigrid method for linear elasticity, SIAM Journal on Scientific Computing 25 (2) (2003) 385–407.
[35] J.K. Kraus, Algebraic multigrid based on computational molecules, 2. Linear elasticity problems, SIAM Journal on Scientific Computing 30 (1) (2008) 505–524.
[36] J. Ruge, A. Brandt, A multigrid approach for elasticity problems on ''thin'' domains, in: S.F. McCormick (Ed.), Multigrid Methods: Theory, Applications, and Supercomputing, Marcel Dekker Inc., New York, 1988, pp. 541–555.
[37] V. Mikulinsky, Multigrid treatment of thin domains, SIAM Journal on Scientific and Statistical Computing 12 (4) (1991) 940–949.
[38] I.H. Shames, C.L. Dym, Energy and Finite Element Methods in Structural Mechanics, Hemisphere Publishing Corporation, New York, 1985.
[39] E. Kreyszig, Advanced Engineering Mathematics, 8th ed., John Wiley & Sons, New York, 1999.
[40] Y.-q. Long, et al., Generalized conforming plate bending elements using point and line compatibility conditions, Computers and Structures 54 (4) (1995) 717–723.